



# NUMERICAL ANALYSIS OF WIND TURBINE DIFFUSER WITH DIFFERENT FLANGE ANGLES

**RENUKA PRASAD Y**

PG Scholar  
Dept. of Mechanical Engineering  
MVJ College of Engineering Bangalore-560067  
Karnataka, India  
E-mail: [renukaprasad.y@gmail.com](mailto:renukaprasad.y@gmail.com)

**Dr. Y.VIJAYAKUMAR**

Professor & Principal  
Mechanical Engineering  
Sri Sairam College of Engineering  
Bangalore -108  
Email: [principal@sairamce.edu.in](mailto:principal@sairamce.edu.in)

**CHANDRASEKHAR G L**

Associate Professor,  
Dept. of Mechanical Engineering  
MVJ College of Engineering Bangalore-560067  
Karnataka, India  
E-mail: [chandrashakar.gotur@gmail.com](mailto:chandrashakar.gotur@gmail.com)

## ABSTRACT

This analysis shows an advancement and investigation of 3-D wind turbine diffuser model with various flange angles. The 3-D models are produced by utilizing Solid Edge ST9 and analysis investigation has been completed by using ANSYS FLUENT 14.5. This analysis concentrates on the impact of flange angles as a changed parameter on velocity at diffuser passage. All models have same measurements in diffuser length, entrance distance across, leave width and flange height but differ in flange angle. Flange angle of these models are varied from  $-25^{\circ}$  to  $+25^{\circ}$ , where flange angles were measured to vertical axis.

The numerical simulation demonstrates the made vortices behind flange that cause pressure drop which expands mass stream rate at the entrance of the diffuser. The outcomes also show that the angle at  $+5^{\circ}$  is the optimum angle that accelerates flow at diffuser entrance. The expansion of velocity at this optimum flange angles is higher than the instance of ordinary angle, where wind turbine can achieve more efficiency compared with the normal flange angle.

**Keywords** – Wind Turbine, Diffuser Model, Flange Angle, CFD Analysis

## I. INTRODUCTION

Burning of gigantic amounts of petroleum products worldwide for power creation causes a various ecological issue, for example, corrosive rain, brown haze and environmental change because of non-renewable energy source ignition's discharges.

Lately, there are worldwide endeavors to lessen the overall reliance on petroleum derivatives. Thus, the worldwide mindfulness has prompted a stirring of enthusiasm for sustainable power source innovation as cleaner power era techniques. The wind energy is a potential power source. In this way, there is an expansion of assembling rate of wind generator turbines with various sizes. One of the contrasts amongst extensive and little scale wind turbines is that little scale wind turbines are for the most part found where the power is required, frequently inside a constructed situation, as opposed to where the wind is generally great. To yield a sensible power yield from a little scale, the turbines need to enhance their energy catch, especially at low wind speeds.



## II. Literature Review

It is realized that created power by wind turbines is corresponding to the cubic energy of the occurrence wind speed any little increment in incident wind causes a large increment in the energy output. Therefore, analysts attempting to increase wind speed locally at wind turbine. Shrouded or ducted wind turbine is one of the imperative utilized method to enhance power from wind turbine.

The possibility of DAWT was proposed by Lilly and Rainbird [1]. They performed a theoretical review to acquire the gain of created power yield from a completely ducted path wind turbine that was 65% of most extreme power yield of the perfect uncovered wind turbine. Experiment and computational investigations were performed in 1980s by Foremen [2] Forman et al. Examine a specialized and financial learn about diffuser augmented wind turbine "DAWT". The review acquired critical power growth from DAWT moving toward twice of energy produced by uncovered wind turbine. The expansion of energy delivered because of low weight at diffuser leave that pumps substantially bigger measures of air through a DAWT than an ordinary wind turbine. Gilbert et al [3] concentrate the parameters that impact on the execution of the diffuser framework and analyzed it in the wind burrow. Their original of DAWT given about double the energy of an ordinary wind vitality change framework with same wind turbine width and wind speed and wind velocity and maximum augmentation ratio reaches 3. Ohya et al. discovered hollow- structure diffuser is as viable as the shrouded form wind turbine for gathering and quickening the wind Likewise, they found when utilizing a flange of proper height appended to the external periphery of the diffuser leave, a wonderful increment in wind speed. Aly M et al [5] performed about an improvement and investigation of 2-D axisymmetric CFD model of flanged diffuser that utilized as a packaging for grew little wind turbine to increase generated power. In this analysis 3-D models are produced by utilizing Solid Edge ST9 and analysis investigation has been completed by using ANSYS FLUENT 14.5.

## III. Governing equations

In this problem K-ε turbulence model is used which is expressed by elliptical Navier-Stokes PD equations. The flow is assumed to be steady, turbulent, 3-dimensional incompressible and air is considered as the working fluid.

## IV. Turbulence equation

### K - Equation

$$\frac{\partial(\rho u K)}{\partial x} + \frac{\partial(\rho v K)}{\partial y} = \frac{\partial}{\partial x} \left[ \left( \mu + \frac{\mu_t}{\sigma_k} \right) \frac{\partial K}{\partial x} \right] + \frac{\partial}{\partial y} \left[ \left( \mu + \frac{\mu_t}{\sigma_k} \right) \frac{\partial K}{\partial y} \right] - g \frac{\mu_t}{Pr_t} \frac{\partial \rho}{\partial x} + \mu_t \left\{ 2 \left[ \left( \frac{\partial u}{\partial x} \right)^2 + \left( \frac{\partial v}{\partial y} \right)^2 \right] + \left( \frac{\partial u}{\partial y} + \frac{\partial v}{\partial x} \right)^2 \right\} - \rho \epsilon$$

### ε-equation

$$\frac{\partial(\rho u \epsilon)}{\partial x} + \frac{\partial(\rho v \epsilon)}{\partial y} = \frac{\partial}{\partial x} \left[ \left( \mu + \frac{\mu_t}{\sigma_\epsilon} \right) \frac{\partial \epsilon}{\partial x} \right] + \frac{\partial}{\partial y} \left[ \left( \mu + \frac{\mu_t}{\sigma_\epsilon} \right) \frac{\partial \epsilon}{\partial y} \right] - C_{1\epsilon} g \frac{\epsilon}{K} \frac{\mu_t}{Pr_t} \frac{\partial \rho}{\partial x} + C_{1\epsilon} \frac{\epsilon}{K} \mu_t \left\{ 2 \left[ \left( \frac{\partial u}{\partial x} \right)^2 + \left( \frac{\partial v}{\partial y} \right)^2 \right] + \left( \frac{\partial u}{\partial y} + \frac{\partial v}{\partial x} \right)^2 \right\} - C_{2\epsilon} \rho \frac{\epsilon^2}{K}$$

### Boundary conditions

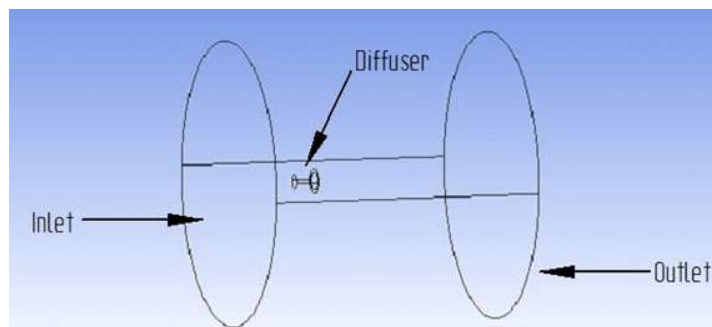


**Figure 1:** Line diagram of diffuser enclosed with domain

Due to symmetric nature of condition flow is considered to be three-dimensional flow (3D) in the  $x$ - $y$ - $z$  plane. Boundary conditions are a very important step in numerical solution. It depends on some assumptions. Schematic diagram of diffuser inside the cylindrical domain as shown above. In which for inlet velocity  $u = u_{\infty}$  (free stream velocity), for outlet flow is compressible which is flow in = flow out, for diffuser wall and domain wall no slip boundary condition is used. [4] proposed a principle in which another NN yield input control law was created for an under incited quad rotor UAV which uses the regular limitations of the under incited framework to create virtual control contributions to ensure the UAV tracks a craved direction. Utilizing the versatile back venturing method, every one of the six DOF are effectively followed utilizing just four control inputs while within the sight of un demonstrated flow and limited unsettling influences. Elements and speed vectors were thought to be inaccessible, along these lines a NN eyewitness was intended to recoup the limitless states. At that point, a novel NN virtual control structure which permitted the craved translational speeds to be controlled utilizing the pitch and the move of the UAV. At long last, a NN was used in the figuring of the real control inputs for the UAV dynamic framework. Utilizing Lyapunov systems, it was demonstrated that the estimation blunders of each NN, the spectator, Virtual controller, and the position, introduction, and speed following mistakes were all SGUUB while unwinding the partition Principle.

### V. Geometry

3-D models are produced by utilizing Solid Edge ST9, all models have same measurements in diffuser length, entrance distance across, leave width and flange height but differ in flange angle. Flange angle of these models are varied from  $-25^{\circ}$  to  $+25^{\circ}$ , where flange angles were measured to vertical axis. Schematic diagram of flanged diffuser in test section as shown below.

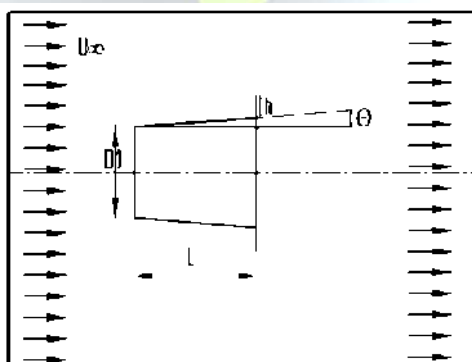


**Figure 2:** Schematic diagram of diffuser in test section

Where,

$U_{\infty}$  = free stream velocity = 4.5 m/s

$D1$  = 1 m



$$h = 0.25 \text{ m L} =$$
$$= 1.5 \text{ m } \Theta =$$
$$4^{\circ}$$

3-D models are developed from Solid Edge ST9 as shown below. Flange angle of these models are varied from  $-25^{\circ}$  to  $+25^{\circ}$ . These models are imported to ANSYS FLUENT 14.5 using .iges file format. And create a cylindrical dominie on it for further calculation. Which as shown in figure



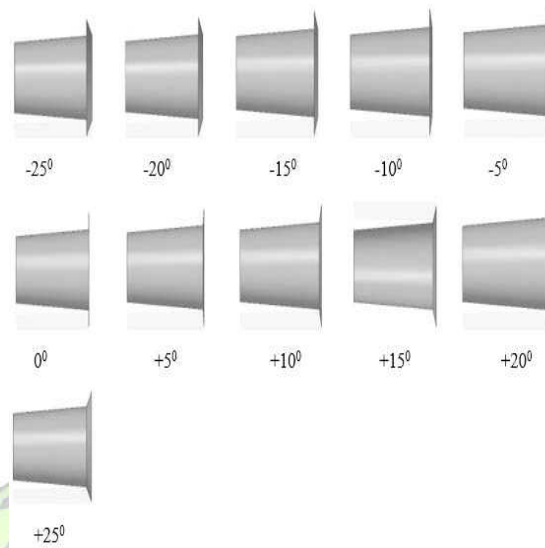


Figure 3: 3-D models for -25° to +25° of flange angle

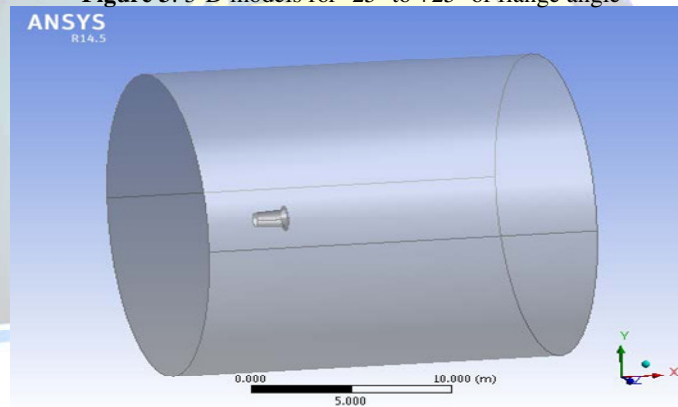
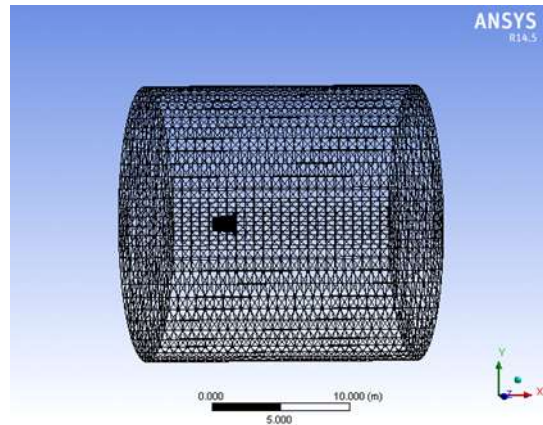


Figure 4: Flanged diffuser with cylindrical domain

## VI. Meshing

The problem domain divided in to finet number of nodes and generates a mesh to create a number of cells. The cell number and size of mesh depending up on number of nodes in domain and mesh type which may be structural or unstructured. In this investigation the domain is divided in quadrilateral cells. The number of elements in the mesh generated is 376994 and number of nodes in the mesh generated is 69794



**Figure 5:** Complete view of meshed with domain

### VII. Physical setup

Inlet	
Type	Velocity Inlet
Magnitude	15m/s
Outlet	
Type	Pressure Outlet
Magnitude	0 bar
Wall	
Type	Stationary
Convergence Criteria	
Continuity	1e-7
X Velocity	1e-11
Y Velocity	1e-11
Z Velocity	1e-11
K	1e-7
$\epsilon$	1e-7
Turbulence Model	
Type	K- $\epsilon$ Model
Specific Methods	
Turbulence intensity	2.6%
Hydraulic diameter	21m

**Table 1:** Physical setup for CFD analysis

### VIII. Numerical Solutions

The CFD FLUENT provides a detailed information and visualization of air flow over diffuser. These outcomes approve the wonder of speed increment when flange is utilized at diffuser exit. Velocity of stream field is acquired from contours.

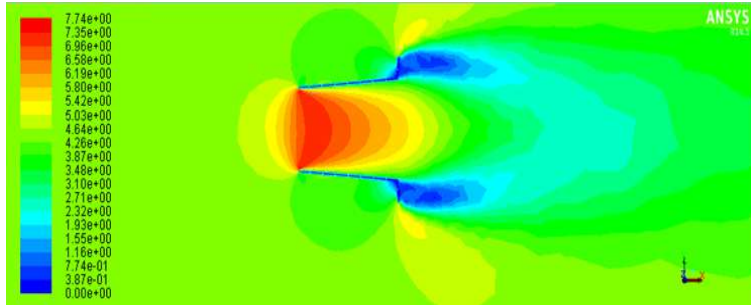


Figure 6: Filled view of Velocity magnitude contour of flow field at flange angle  $\theta = +5^\circ$

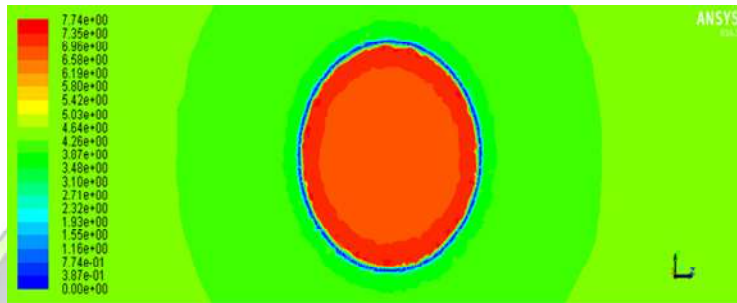


Figure 7: Velocity at inlet of diffuser in  $+5^\circ$  of flange angle

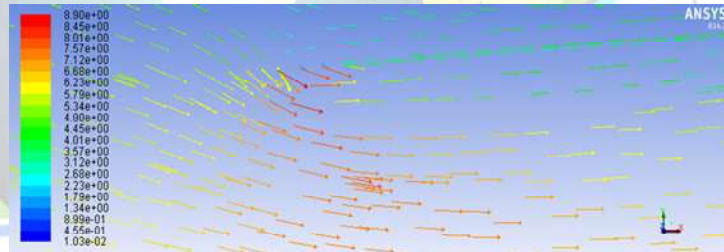


Figure 8: Vector view at diffuser entrance in  $+5^\circ$  of flange angle

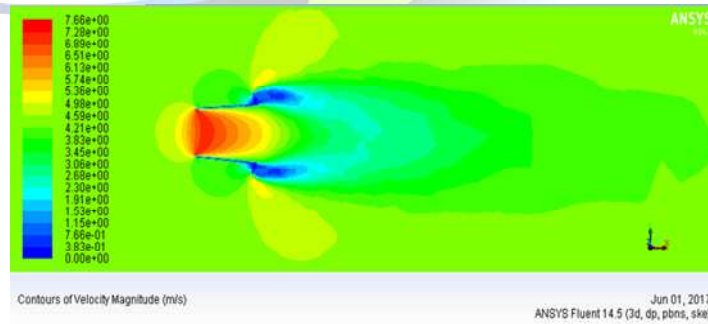


Figure 9: Filled view of Velocity magnitude contour of flow field at flange angle  $\theta = -25^\circ$

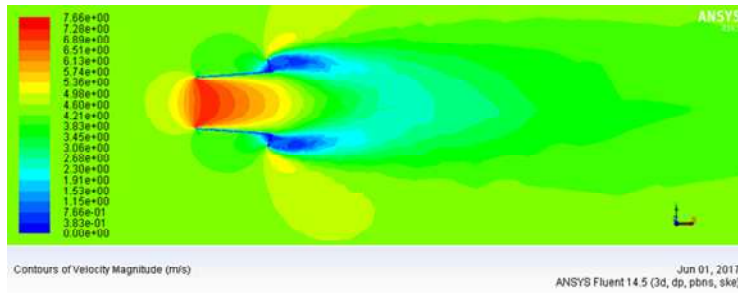


Figure 10: Filled view of Velocity magnitude contour of flow field at flange angle  $\theta = -20^\circ$

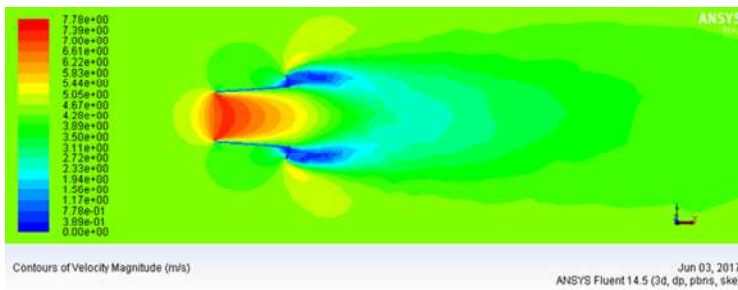


Figure 11: Filled view of Velocity magnitude contour of flow field at flange angle  $\theta = -15^\circ$

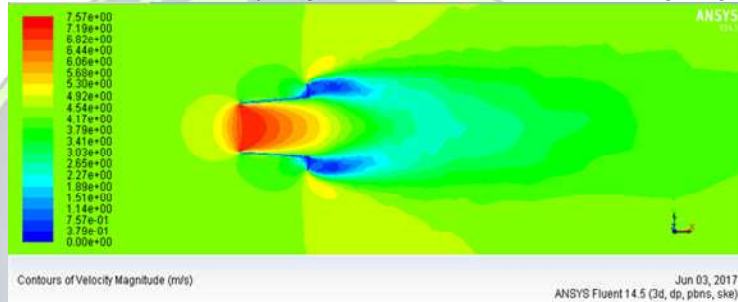


Figure 12: Filled view of Velocity magnitude contour of flow field at flange angle  $\theta = -10^\circ$

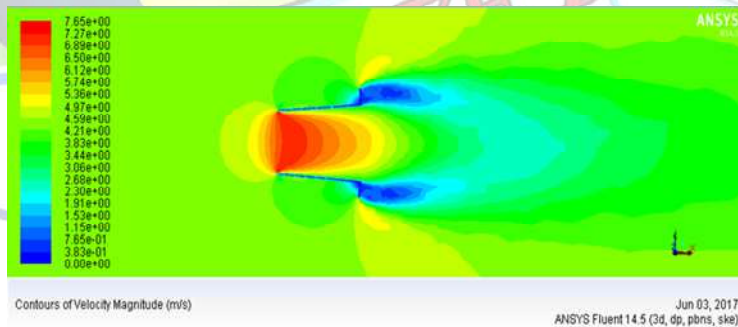


Figure 13: Filled view of Velocity magnitude contour of flow field at flange angle  $\theta = -5^\circ$

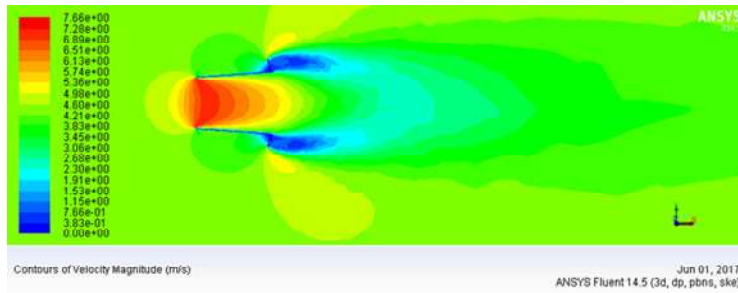


Figure 14: Filled view of Velocity magnitude contour of flow field at flange angle  $\theta = 0^\circ$

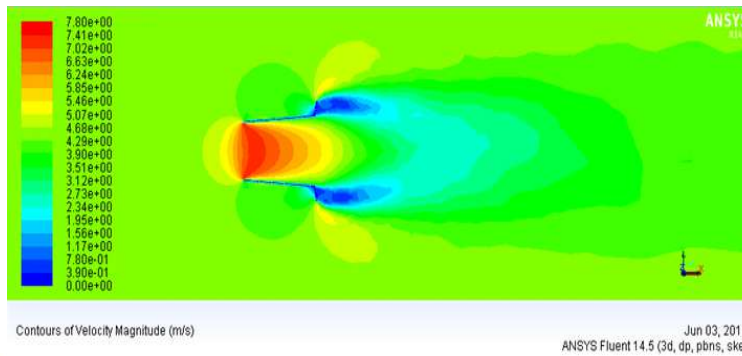


Figure 15: Filled view of Velocity magnitude contour of flow field at flange angle  $\theta = +10^\circ$

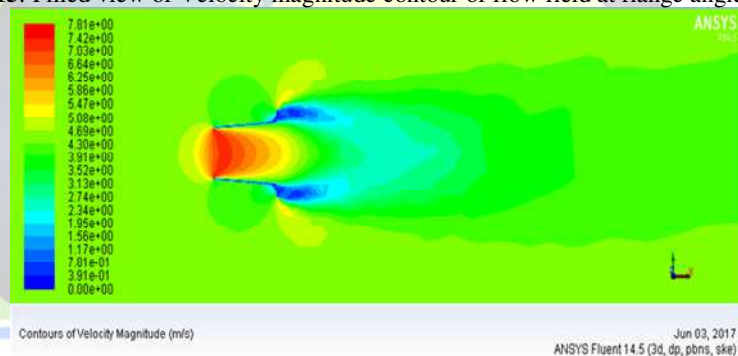


Figure 16: Filled view of Velocity magnitude contour of flow field at flange angle  $\theta = +15^\circ$

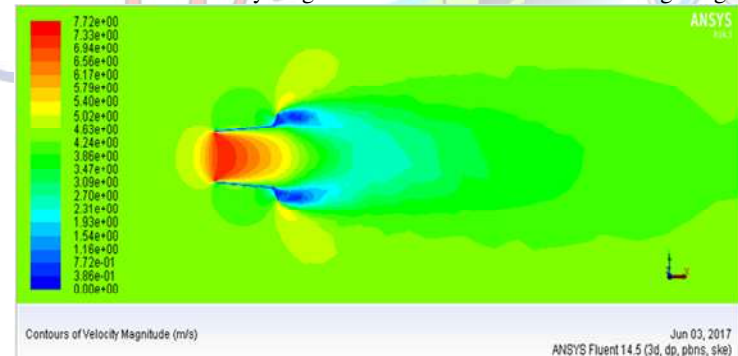


Figure 17: Filled view of Velocity magnitude contour of flow field at flange angle  $\theta = +20^\circ$

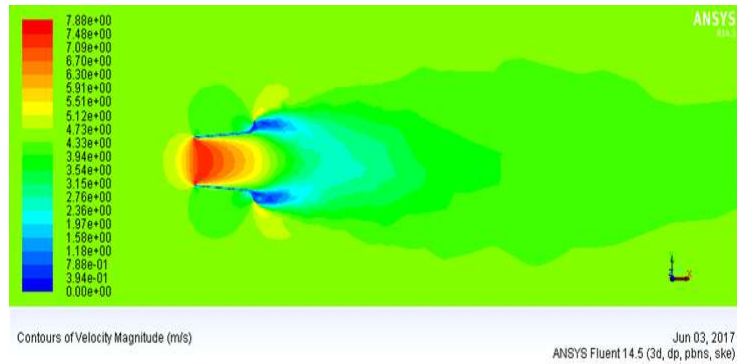


Figure 18: Filled view of Velocity magnitude contour of flow field at flange angle  $\theta = +25^\circ$

### IX. Results and Discussion

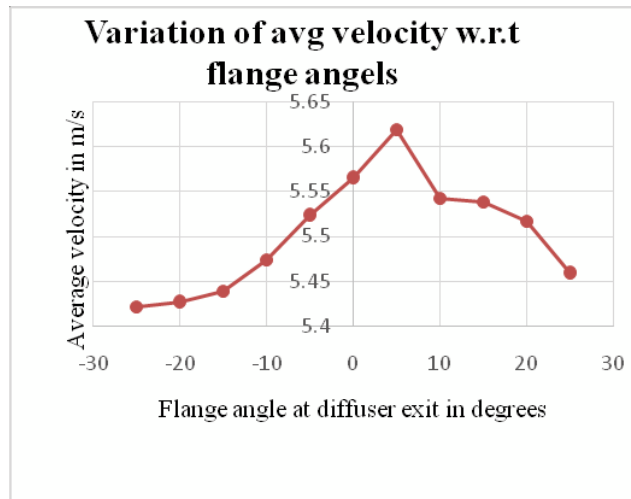
The 3D wind turbine diffuser model was computationally analyzed through ANSYS FLUENT 14.5 and results are plotted

#### Variation of average velocity with respect to flange angles at diffuser exit

Variation of average velocity w.r.t flange angle at diffuser exit is tabulated for following dimension. Average velocity can be calculating by using ANSYS function calculator = 1.5 m,  $D1 = 1$  m,  $\theta = 40$ ,  $h = 0.25$  m,  $V_\infty = 4.5$  m/s All models have same measurements in diffuser length, entrance distance across, leave width and flange height but differ in flange angle. Flange angle of these models are varied from  $-25^\circ$  to  $+25^\circ$ , where flange angles were measured to vertical axis.

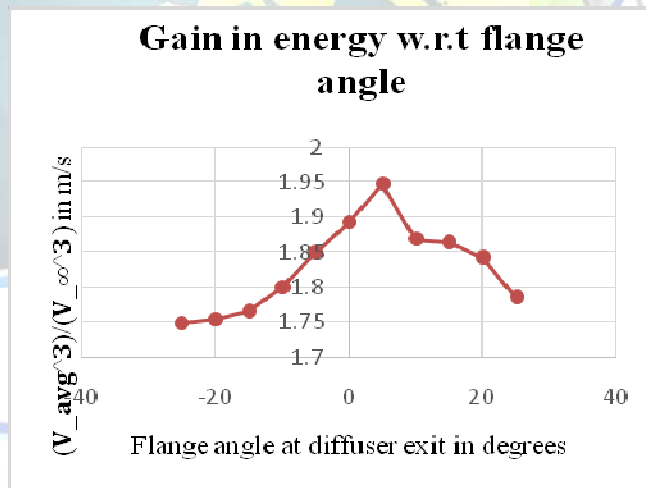
Flange angle in $\theta$	Average velocity In diffuser inlet ( $V_{avg}$ .) in m/s	$V_\infty$ in m/s	in m/s
-250	5.42124	4.5	1.748471
-200	5.42698	4.5	1.75403
-150	5.43849	4.5	1.765214
-100	5.47326	4.5	1.799288
-50	5.52375	4.5	1.849543
00	5.56545	4.5	1.891748
+5	5.61853	4.5	1.946393
+100	5.54234	4.5	1.86828
+150	5.53774	4.5	1.863632
+200	5.51613	4.5	1.8419
+250	5.45921	4.5	1.785467

Table 2: Variation of average velocity w.r.t flange angles



**Figure 19:** Variation of average velocity w.r.t flange angles

Above graph is shows that the average velocity is maximum at diffuser inlet for  $\theta = +5^\circ$  of flange angle. Hence for optimizing the diffuser, we can keep the flange angle as  $+5^\circ$ . Below figure shows the gain in energy with variation of flange angles at diffuser exit. The figure shows the gain in energy is also maximum for flange angle  $\theta = +5^\circ$ .



**Figure 20:** Gain in energy with variation of flange angles at diffuser exit

### X. Conclusion

The present numerical review utilizing ANSYS FLUENT 14.5 package appears the flow attributes inside diffuser model and around it for various flange edges, where the below conclusions are found:

- The present numerical outcomes prove the existence of vortices behind the diffuser flange that causes negative pressure which leads to increase in average velocity of air entering the diffuser.
- The plot of variation of average velocity w.r.t flange angles at diffuser exit depicts the maximum average velocity at flange angle ( $\theta$ ) equals to  $+5^\circ$
- At optimum flange angle of  $+5^\circ$  the expected power increase ratio of 1.946393 was recorded which was more compared to that in normal flange angle (1.891748). This enhances the power generation by 5.4% due to the optimum flange angle.
- The results from this work showed good agreement with the published article on 2D analysis of diffuser [5].



## REFERENCES

ANSYS 14.5 help manual

- [1] Lilley and Rainbird, W. J., "A Preliminary report on the Design and Performance of a Ducted Windmill", College of Aeronautics-1956.
- [2] Foreman, Gillbert, R a Omen "Diffuser Augmentation of Wind turbines", Solar. Energy 20(1978)
- [3] Gilbert, B. L. and Forman, K. M., "Experiments with a Diffuser-Augmented Model Wind Turbine", Journal of Energy Resource Technology, Volume 105, 1983.
- [4] Christo Ananth,"A Novel NN Output Feedback Control Law For Quad Rotor UAV",International Journal of Advanced Research in Innovative Discoveries in Engineering and Applications[IJARIDEA],Volume 2,Issue 1,February 2017,pp:18-26..
- [5]. Aly M. El-Zahaby, A.E. Kabeel, S.S. Elsayed and M.F. Obiaa." CFD Analysis of flow fields for shrouded wind turbine's diffuser model with different flanges angles." Alexandria Engineering journal, (2016)

